Biodiversity and trophic ecology of hydrothermal vent fauna associated with tubeworm assemblages on the Juan de Fuca Ridge

Yann Lelièvre[1,2*], Jozée Sarrazin[1], Julien Marticorena[1], Gauthier Schaal[3], Thomas Day[1], Pierre Legendre[2], Stéphane Hourdez[4], Marjolaine Matabos[1]

[1]*Ifremer, Centre de Bretagne, REM/EEP, Laboratoire Environnement Profond, 29280 Plouzané, France*

[2]*Département de sciences biologiques, Université de Montréal, C.P. 6128, succursale Centre-ville, Montréal, Québec, H3C 3J7, Canada*

[3]*Laboratoire des Sciences de l'Environnement Marin (LEMAR), UMR 6539 9 CNRS/UBO/IRD/Ifremer, BP 70, 29280, Plouzané, France*

[4]*Sorbonne Universités, UPMC Univ. Paris 06, CNRS UMR 7144, Adaptation et Diversité en Milieu Marin, Station Biologique de Roscoff, 29688 Roscoff, France*

Corresponding author

Lelièvre Yann

(1) Département de sciences biologiques, Université de Montréal, C.P. 6128, succursale Centre-ville, Montréal, Québec, H3C 3J7, Canada; (2) Ifremer, Centre de Bretagne, REM/EEP, Laboratoire Environnement Profond, 29280 Plouzané, France.

Telephone number in Canada: +1 514 343 7591

Email address: yann.lelievre@ifremer.fr

Abstract

Hydrothermal vent sites along the Juan de Fuca Ridge in the north-east Pacific host dense populations of *Ridgeia piscesae* tubeworms that promote habitat heterogeneity and local diversity. A detailed description of the biodiversity and community structure is needed to help understand the ecological processes that underlie the distribution and dynamics of deep-sea vent communities. Here, we assessed the composition, abundance, diversity and trophic structure of six tubeworm assemblages, corresponding to different successional stages, collected on the Grotto hydrothermal edifice (Main Endeavour, Juan de Fuca Ridge) at 2196 m depth. Including *R. piscesae*, a total of 36 macrofaunal taxa were identified to the species level. Although polychaetes made up the most diverse taxon, faunal densities were dominated by gastropods. Most tubeworm aggregations were numerically dominated by the polychaete *Amphisamytha carldarei* and gastropods *Lepetodrilus fucensis* and *Depressigyra globulus*. The highest diversities were found in mature tubeworm aggregations, characterized by fairly long tubes. The high biomass of grazers and the high resource partitioning at small scale illustrates the importance of the diversity of free-living microbial communities in the maintenance of the food web. Although symbiont-bearing invertebrates *R. piscesae* represented a large part of the total biomass, the absence of specialized predators on this potential food source suggests that its primary role lies in community structuring. Vent food webs did not appear to be organized through predator-prey relationships. For example, although trophic structure complexity increased with ecological successional stages, showing a higher number of predators in the last stages, the food web structure itself did not change across assemblages. We suggest that environmental gradients provided by the biogenic structure of tubeworm bushes generate a multitude of ecological niches and contribute to the partitioning of nutritional resources, releasing communities from competition pressure for resources, thus allowing species co-existence.

Keywords: Juan de Fuca Ridge; hydrothermal vents; Ridgeia piscesae; community structure; diversity; stable isotopes; food webs.

1. Introduction

Deep-sea hydrothermal vents have developed along mid-ocean ridges and back-arc spreading centres, which are characterized by strong volcanic and tectonic activity. The resulting hydrothermal fluid fosters dense communities of highly specialized fauna that colonize the steep physical and chemical gradients created by the mixing of hot vent fluids with cold seawater. These communities are distributed according to species' physiological tolerance (Childress and Fisher, 1992; Luther et al., 2001), resource availability (De Busserolles et al., 2009; Levesque et al., 2003) and biotic interactions (Lenihan et al., 2008; Micheli et al., 2002; Mullineaux et al., 2000, 2003). Although the fauna are highly dissimilar between oceanic basins (Bachraty et al., 2009; Moalic et al., 2011), hydrothermal communities throughout the world share some ecological similarities including a food web based on chemosynthesis (Childress and Fisher, 1992), low species diversity compared with adjacent deep-sea and coastal benthic communities (Van Dover and Trask, 2000; Tunnicliffe, 1991), high levels of endemism (Ramirez-Llodra et al., 2007), and elevated biomass associated with the presence of large invertebrate species.

The high spatial heterogeneity of environmental conditions in vent ecosystems is amplified by stochastic or periodic temporal variation in hydrothermal activity, influencing the composition (Sarrazin et al., 1999), structure (Marcus et al., 2009; Sarrazin et al., 1997; Tsurumi and Tunnicliffe, 2001) and dynamics (Lelièvre et al., 2017; Nedoncelle et al., 2013, 2015; Sarrazin et al., 2014) of faunal communities. In addition, the complexity of vent habitats is increased by engineer species, whose presence strongly contributes to the modification of the physical (temperature, hydrodynamics processes) and chemical (hydrogen sulfide, methane, oxygen, metals and other reduced chemicals) properties of the environment either by creating three-dimensional biogenic structures (autogenic species) or through their biological activity (allogeneic species) (Jones et al., 1994, 1997). Habitat provisioning and modification by engineer species increases the number of potential ecological niches and, consequently, influences species distribution and contributes to the increase in local diversity (Dreyer et al., 2005; Govenar and Fisher, 2007; Urcuyo et al., 2003). Engineer species promote local diversity through various ecological mechanisms (Bergquist et al., 2003), providing secondary substratum for colonization, a refuge from

predation and unfavourable abiotic conditions or important food sources that enhance the development of macro- and meiofaunal communities (Dreyer et al., 2005; Galkin and Goroslavskaya, 2010; Gollner et al., 2006; Govenar et al., 2005, 2002; Govenar and Fisher, 2007; Turnipseed et al., 2003; Zekely et al., 2006).

Hydrothermal vent food webs are mainly based on local microbial chemosynthesis (Childress and Fisher, 1992), performed by free-living or/and symbiotic chemoautotrophic microorganisms that utilize the chemical energy released in the oxidation of reduced chemicals species (e.g. H_2S, CH_4) present in the hydrothermal fluids (Childress and Fisher, 1992). Several electron donors (e.g. H_2, H_2S, CH_4, NH_4^+, etc.) and electron acceptors (e.g. O_2, NO_3^-, SO_4^{2-}, etc.) can be used by these microorganisms as energy sources, converting inorganic carbon (e.g. CO_2) into simple carbohydrates (Fisher et al., 2007). Chemosynthetic primary production is exported to the upper trophic levels through direct ingestion (primary consumers), or through the presence of intra- or extracellular symbiosis. Upper trophic levels (secondary consumers) are represented by local predators and scavengers feeding on primary consumers and by abyssal species attracted by the profusion of food. Although behavioural observations and stomach content analyses remain limited in these remote deep-sea habitats, stable isotope analyses are widely used to study faunal trophic interactions in these environments (Conway et al., 1994). The emergence of isotopic methods has opened new perspectives in the understanding of food-web functioning and the organization of species diversity within hydrothermal ecosystems around the globe (Bergquist et al., 2007; De Busserolles et al., 2009; Van Dover, 2002; Erickson et al., 2009; Gaudron et al., 2012; Levesque et al., 2006; Levin et al., 2009; Limén et al., 2007; Portail et al., 2016; Soto, 2009; Sweetman et al., 2013). The carbon isotope composition ($\delta^{13}C$) is an indicator of the food assimilated and remains relatively constant during trophic transfers (± 1‰). The kinetics of enzymes involved in the biosynthetic pathways of autotrophic organisms influence the carbon isotope ratio ($^{13}C/^{12}C$), allowing the discrimination between the sources fuelling the community (Conway et al., 1994; Van Dover and Fry, 1989). Nitrogen isotope composition ($\delta^{15}N$) provides information on trophic levels (Michener and Lajtha, 2008) and becomes enriched in heavy isotopes at a rate of ± 3.4‰ at each trophic level. At the community scale, $\delta^{13}C$ and $\delta^{15}N$ signatures of all species in the ecosystem are used to retrace carbon and nitrogen fluxes along the trophic network and, therefore, to reconstitute

115 the food web (Levin and Michener, 2002). Despite the relatively low diversity of the deep-
116 sea community, ample evidence suggests that the deep-sea hydrothermal food-web
117 structure is complex (Bergquist et al., 2007; Portail et al., 2016) including many trophic guilds
118 (Bergquist et al., 2007; De Busserolles et al., 2009) and multiple sources of primary
119 production (Van Dover and Fry, 1994).
120
121 Active hydrothermal vents on the Juan de Fuca Ridge (north-east Pacific) are colonized by
122 populations of the siboglinid polychaete *Ridgeia piscesae* (Urcuyo et al., 2003) forming dense
123 faunal assemblages in areas of high to low fluid flux activity. Diverse heterotrophic faunal
124 species inhabit these tubeworm bushes, with a dominance of polychaete and gastropod
125 species (Bergquist et al., 2007; Govenar et al., 2002; Marcus et al., 2009; Tsurumi and
126 Tunnicliffe, 2001, 2003). To date, few studies have described the communities associated
127 with the *R. piscesae* tubeworm assemblage of the Main Endeavour vent field, either in terms
128 of diversity (Bergquist et al., 2007; Sarrazin et al., 1997) or trophic ecology (Bergquist et al.,
129 2007). Six distinct faunal assemblages exhibiting patchy distributions have been identified on
130 the Smoke & Mirrors hydrothermal edifice, and represent different successional stages
131 (Sarrazin et al., 1997). Assemblages I and II are characterized by pioneer *Paralvinella*
132 *palmiformis* polychaete species that colonize new unstable high-temperature surfaces and
133 whose biological activity tends to stabilize the substratum (Juniper et al., 1992; Sarrazin et
134 al., 1997). Assemblage III is marked by dense aggregations of *P. palmiformis* and the
135 colonization of high densities of gastropods *Lepetodrilus fucensis*, *Depressigyra globulus* and
136 *Provanna variabilis* (Sarrazin et al., 1997). Assemblage IV is characterized by the growth of *R.*
137 *piscesae*, leading to assemblage V associated with a more complex physical structure and
138 consequently with an increase in local diversity, density and biomass (Bergquist et al., 2003;
139 Sarrazin et al., 1997; Tsurumi and Tunnicliffe, 2003). Finally, assemblage VI characterizes a
140 senescent phase in which *R. piscesae* gradually dies and its associated species disappear,
141 with a dominance of filamentous bacteria and detritivores (Sarrazin et al., 1997). A
142 successional model proposes that the transition between the first two assemblages is mostly
143 driven by biotic interactions, and those between the other assemblages are principally
144 initiated by modifications in hydrothermal activity (Sarrazin et al., 1997). Within a single
145 assemblage of *R. piscesae* tubeworm from diffuse flow vent environments of Easter Island

(Main Endeavour, Juan de Fuca Ridge), Bergquist *et al*. (2007) reported that tubeworm-generated habitats supported a diverse community, with a complex local food web.

Since 2011, a camera installed on the *Ocean Networks Canada* cabled observatory has been recording high-resolution imagery of a *R. piscesae* tubeworm assemblage and its associated fauna on the active Grotto hydrothermal edifice (Main Endeavour, Juan de Fuca Ridge). The processing of this data provided new insights on the influence of astronomic and atmospheric forcing on vent faunal dynamics (Lelièvre et al., 2017), but thorough knowledge of the faunal communities observed by the camera is still needed to understand and interpret the temporal patterns and their underlying mechanisms. However, although video imagery is useful for investigating the spatial distribution of communities (Cuvelier et al., 2011; Sarrazin et al., 1997), species behaviour (Grelon et al., 2006; Matabos et al., 2015) and temporal dynamics of a sub-set of the species (Cuvelier et al., 2014; Lelièvre et al., 2017), direct sampling is an essential and complementary approach for determining faunal composition, abundance and species diversity and functioning (Cuvelier et al., 2012). In this context, the objectives of the present study were: (*i*) to identify the composition and structure of six faunal assemblages associated with *R. piscesae* tubeworm bushes on the Grotto hydrothermal edifice, specifically with respect to density, biomass and species diversity; (*ii*) to characterize the trophic structure of these biological communities and (*iii*) to assess how diversity and trophic relationship vary over the different successional stages.

2. Materials and Methods

2.1. Geological setting

The Juan de Fuca Ridge (JdFR) (Fig. 1a) is an intermediate spreading-rate ridge between the Pacific and Juan de Fuca plates in the north-east Pacific Ocean. The Endeavour Segment (47°57’N, 129°06’W) (Fig. 1b) constitutes a ~ 90 km long section of the JdFR, bounded to the north by the Middle Valley site and to the south by the Cobb Segment. It is characterized by a 500–1000 m wide axial valley whose walls reach up to 200 m in height (Delaney et al., 1992). The five major vent fields – Sasquatch, Salty Dawg, High Rise, Main Endeavour (MEF) and Mothra – found on the Endeavour axial valley are separated by 2–3 km.

The MEF (Fig. 1c) is the most intense and active of the five hydrothermal fields, with the presence of high-temperature (370-390°C), actively venting sulfide edifices and diffuse low-temperature (10-25°C) venting areas (Delaney et al., 1992; Kelley et al., 2012). Within the MEF, Grotto (47°56.958'N, 129°5.899'W, Fig. 1d) is an active hydrothermal sulfide vent cluster (15 m long by 10 m wide by 10 m high) located at 2196 m depth that forms an open cove to the north. This edifice is characterized by high short-term variation in heat flux, but a relative stability in years with low seismic activity (Xu et al., 2014). Like many other MEF hydrothermal edifices, the site is largely colonized by dense assemblages of *R. piscesae* (Polychaeta, Siboglinidae) with their associated fauna (Sarrazin et al., 1997).

2.2. Faunal assemblage sampling

Sampling took place during the ONC oceanographic cruises *Wiring the Abyss 2015 and 2016* from 25 August to 14 September 2015 on the R/V *Thomas G. Thompson*, and from 10 May to 29 May 2016 on the E/V *Nautilus*, respectively. Using the remotely operated vehicles (ROVs) *Jason* and *Hercules*, three assemblages of *R. piscesae* tubeworms and their associated fauna were sampled each year at different locations on the Grotto hydrothermal edifice (n=6; S1 to S6, Fig. 2). For each sample, a checkerboard of 7 x 7 mm squares was first placed on each tubeworm assemblage to estimate the surface area. Then, the first suction sample was taken to recover the mobile fauna, followed by collection of tubeworms and their associated fauna, which were placed in a "bio-box" using the ROV's mechanical arm. A final suction sample on the bare surface was performed to recover the remaining fauna. The final sampled surface was filmed with the ROV camera to estimate its surface using imagery (see protocol in Sarrazin *et al*. 1997 (Sarrazin et al., 1997)).

2.3. Sample processing

2.3.1. Sample processing and identification

On board, all faunal samples were washed over stacked sieves (250 µm, 63 µm and 20 µm mesh sizes). Macrofaunal specimens (>250 µm) were preserved in 96 % ethanol and meiofauna (<63 µm) in 10 % seawater formalin. In the laboratory, bushes of *R. piscesae* were thoroughly disassembled and each tube was washed and sieved a second time. All associated macrofaunal organisms were sorted, counted and identified to the lowest

possible taxonomic level. Specimens whose identification was unclear were sent to experts for identification and/or description. When available, trophic guilds from the literature (symbiont host, bacterivore, scavenger/detritivore or predator) were assigned to each vent species. For species with unknown diets, the assignment was based on trophic guilds identified from closely related species (within the same family).

2.3.2 Habitat complexity and biomass

For each tubeworm assemblage, the density measured in number of individuals per square meter (ind m^{-2}) was calculated. In addition to the surface they occupy, *R. piscesae* tubes create a three-dimensional (3D) structure for other vent animals to colonize. An estimation of the volume of each assemblage provided a proxy for habitat complexity. For this, in each sample, 10 % of the tubeworm tubes were randomly selected and measured. Assuming that the tubes are erected vertically, sampling volume was estimated by multiplying the mean tube length by the sampled surface area. Final densities are therefore expressed per m^3 to account for this 3D space. Biomass estimates were obtained for a random sample of 3 to 10 individuals of each species. The total dry mass (DM) of each species corresponds to the mass obtained after drying each individual at 80°C for 48 h; the ash-free dry mass (AFDM) was obtained after combustion in a muffle furnace at 500°C for 6 h. Absolute biomass of each species was calculated by multiplying the relative biomass by the abundance of each species.

2.3.3. Stable isotope processing

Sample preparation for stable isotope analyses was specimen size-dependent. For large specimens, muscle tissue was dissected and used for stable isotope analyses. In the case of intermediate-size specimens, the gut content was removed. For small taxa, entire individuals were analysed or pooled to reach the minimum required mass for isotopic analysis. Samples were freeze-dried and ground into a homogeneous powder using a ball mill or agate mortar. About 1.3-1.4 mg of the powder was precisely measured in tin capsules for isotope analysis. For species containing carbonates (i.e. gastropods, ostracods, amphipods, etc.), individuals were acidified to remove inorganic carbon. Acidification was carried out by the addition of 0.1 M HCl. The sample was then dried at 60°C for 24 h under a fume extractor to evaporate the acid. Five replicates per species were analysed. Carbon and nitrogen isotope ratios were

239 determined using a Thermo Scientific FLASH EA 2000 elemental analyser coupled with a
240 Thermo Scientific Delta V Plus isotope ratio mass spectrometer. Values are expressed in δ
241 (‰) notation relative to Vienna Pee Dee Belemnite and atmospheric N_2 as international
242 standards for carbon and nitrogen, respectively, according to the formula: $\delta^{13}C$ or $\delta^{15}N$ =
243 $[(R_{sample}/R_{standard})-1] \times 10^3$ (in ‰) where R is $^{13}C/^{12}C$ or $^{15}N/^{14}N$. Analytical precision based on
244 repeated measurements of the same sample was below 0.3‰ for both $\delta^{13}C$ and $\delta^{15}N$.
245

246 ### 2.4. Statistical analyses

247 In the present study, *R. piscesae* was regarded as a habitat builder and thus discarded from
248 the statistical analyses. Species-effort curves were computed for each faunal sample
249 collected to assess the robustness of the sampling effort. Local diversity (i.e. α diversity) was
250 estimated for each tubeworm assemblage from several complementary indices (Gray, 2000)
251 using the vegan package in R (Oksanen et al., 2017): species richness (S), exponential
252 Shannon entropy (D), Simpson's (1-λ') indices of species diversity and Pielou's evenness
253 index (J').
254

255 ## 3. Results

256 ### 3.1. Species-effort curves, tubeworm complexity and diversity

257 The rarefaction curves (Fig. 3) showed that, overall, the collected samples (S1 to S6) gave a
258 fairly good representation of the species diversity on the Grotto hydrothermal edifice. In
259 2015, sample S2 (24 taxa, excluding *R. piscesae*) and S3 (31 taxa) rarefaction curves seemed
260 to reach a plateau. S1 cumulated a total of 28 macrofaunal taxa. The samples from year
261 2016 exhibited lower species richness and did not reach an asymptote. Samples S4 and S5
262 had a macrofaunal species richness of 19 taxa, while only 14 taxa were found in sample S6
263 (Fig. 3).
264

265 The volumes of the samples were used as an approximate measure of habitat complexity of
266 the 3D structures of the *R. piscesae* assemblages. Samples S1 and S3 showed similar
267 patterns, with sampling surfaces of 12.36 and 11.92 dm^2 and mean tube lengths of
268 17.24 ± 6.38 and 17.89 ± 5.69 cm, respectively (Table 1). Therefore, S1 and S3 were
269 characterized by a similar degree of complexity, with a volume of 21.31 and 21.33 dm^3.

Sample S2 displayed a sampling area of less than half of that of S1 and S3 (6.33 dm^2) and a mean tube length of 8.16 ± 2.14 cm with an estimated resulting volume of 5.16 dm^3. Samples S4 to S6 were substantially smaller than S1, S2 and S3, with a sampling surface between 1.22 and 1.59 dm^2. *R. piscesae* tubes were short in samples S4 and S5 leading to a sampling volume of 0.7 and 0.86 dm^3 respectively (Table 1). Sample S6 displayed tube lengths similar to S2 leading to a sampling volume of 1.02 dm^3 (Table 1).

Alpha diversity measures showed that S3 displayed the highest diversity (Shannon D = 6.053; 1-λ' = 0.778), slightly greater than S2 (D = 5.398; 1-λ'= 0.749) and S1 (D = 5.377; 1-λ'= 0.728) (Table 1). The lowest diversity values were observed in S5 (D = 4.348; 1-λ' = 0.697), S6 (D = 3.998; 1-λ' = 0.633) and S4 (D = 2.605; 1-λ' = 0.550). The S2 and S3 samples showed a more even distribution (J') of individuals among taxa than the other assemblages. In contrast, S4 had the lowest evenness (J'= 0.325) (Table 1). Species richness was significantly correlated with *R. piscesae* tube length (R^2_{adj} = 0.60, *p-value* = 0.042).

3.2. Composition and structure of Grotto vent communities

The species lists and abundances for each sample collected within the Grotto hydrothermal edifice are provided in Table 2. A total of 148 005 individuals representing 35 macrofaunal taxonomic groups were identified in the six *R. piscesae* assemblages (S1 to S6) sampled on the Grotto edifice. Overall, gastropods (5 taxa) and polychaetes (19 taxa) respectively accounted for 61.51 ± 16.9 % and 29.06 ± 13.06 % of the total macrofaunal abundance. The numerically most abundant species were the gastropods *L. fucensis* and *D. globulus* as well as the polychaete *Amphisamytha carldarei* representing respectively 33.95 ± 7.58 %, 24.54 ± 15.68 % and 15.08 ± 13.57 % of the total abundance. The highest macrofaunal densities were observed in samples S4 (19 364 286 ind m^{-3}), S5 (7 461 628 ind m^{-3}), S2 (5 196 318 ind m^{-3}) and S3 (3 143 241 ind m^{-3}), whereas S6 and S1 had the lowest densities with 1 607 843 ind m^{-3} and 1 523 932 ind m^{-3}, respectively. The foundation species *R. piscesae* represented a large part of the total biomass, with a mean of 69.3 ± 15.7 % of the total biomass, followed by the gastropods *L. fucensis* (14.96 ± 4.05 %) and *D. globulus* (6.76 ± 8.34 %). A high percentage (30 %) of the species were only found in 1 or 2 samples.

More specifically, S1 was dominated by gastropod species such as *L. fucensis* (617 785 ind m^{-3}; 12.48 % of total biomass), *D. globulus* (156 265 ind m^{-3}; 1.12 % of total biomass) and *P. variabilis* (27 452 ind m^{-3}; 2.25 % of total biomass) (Table 2). High densities contrasted with low biomass were also observed for the ampharetid polychaete *A. carldarei* and the syllid polychaete *Sphaerosyllis ridgensis*. S2 was also dominated by *L. fucensis*, *D. globulus* and *A. carldarei*, with, however, a high proportion of ostracods *Euphilomedes climax* (475 388 ind m^{-3}; 0.10 % of total biomass) (Table 2). S3 was largely dominated by *A. carldarei* (1 073 511 ind m^{-3}; 1.84 % of total biomass) and, to a lesser extent, was almost equally dominated by *L. fucensis* (702 438 ind m^{-3}; 11.53 % of total biomass) and *D. globulus* (619 784 ind m^{-3}; 2.86 % of total biomass). Polychaetes were also dominant, with the presence of *S. ridgensis* (52 414 ind m^{-3}; <0.001 % of total biomass), the dorvilleid *Ophryotrocha globopalpata* (40 319 ind m^{-3}; <0.001 % of total biomass) and the maldanid *Nicomache venticola* (7079 ind m^{-3}; 1.09 % of total biomass). There were high densities of *P. variabilis* (138 678 ind m^{-3}; 6.78 % of total biomass), the solenogaster *Helicoradomenia juani* (172 011 ind m^{-3}; 0.14 % of total biomass), the acarida *Copidognathus papillatus* (150 633 ind m^{-3}; <0.001 % of total biomass), the ostracod *Xylocythere sp. nov*. (82 419 ind m^{-3}; <0.001 % of total biomass) and the pycnogonid *Sericosura verenae* (22 644 ind m^{-3}; 0.84 % of total biomass) (Table 2). S4 was dominated by *L. fucensis* (7 700 000 ind m^{-3}; 19.43 % of total biomass) and *D. globulus* (9 195 714 ind m^{-3}; 13.02 % of total biomass) and, to a lesser extent, by the alvinellid polychaete *P. palmiformis* (591 429 ind m^{-3}; 6.78 % of total biomass) (Table 2). S5 was also dominated by *L. fucensis* and *D. globulus*, followed by *E. climax* (624 419 ind m^{-3}; <0.001 % of total biomass) and *P. variabilis* (594 186 ind m^{-3}; 10 % of total biomass) (Table 2). Finally, S6 was also dominated *L. fucensis* and *D. globulus* and, to a lesser extent, by *A. carldarei* (86 275 ind m^{-3}; 0.07 % of total biomass) and the alvinellid polychaete *Paralvinella pandorae* (63 725 ind m^{-3}; <0.001 % of total biomass) (Table 2).

3.4. $\delta^{13}C$ and $\delta^{15}N$ isotopic composition

$\delta^{13}C$ values of the vent fauna ranged from −33.4 to −11.8 ‰ among the different samples (Fig. 4). More specifically, $\delta^{13}C$ values ranged from −33.4 to −13.5 ‰ for S1, from −33.4 to −15.4 ‰ for S2 and from −32.4 to −14.7 ‰ for S3. Samples from S4, S5 and S6 displayed slightly narrower $\delta^{13}C$ ranges, varying from −30.3 to −12.5 ‰, from −31.3 to −14.8 ‰ and

from −32.3 to −11.8 ‰, respectively; most species were enriched in ^{13}C relative to the S1, S2 and S3 samples (Fig. 4). Overall, the gastropod *P. variabilis* (species #2) was the most depleted in ^{13}C with values around −32.2‰ (± 1.2 ‰). In contrast, *R. piscesae* siboglinids (species #1) showed the highest $\delta^{13}C$ values, with constant values around −14.7 ‰ (± 1.0 ‰). The range of $\delta^{15}N$ values in faunal assemblages varied between −8.5 and 9.4 ‰ (Fig. 4). More specifically, S1 values ranged from 0.3 to 8.4 ‰, S2 from 0.4 to 9.2‰, S3 from −2.7 to 8.3‰, S4 from −1.3 to 8.7 ‰, S5 from −1.1 to 6.4 ‰ and S6 from −8.5 to 9.4 ‰ (Fig. 4). Overall, 15 species showed a $\delta^{15}N > 5$ ‰ in S1, S2 and S3 assemblages but only 4 species were over 5 ‰ in $\delta^{15}N$ in S4, S5 and S6. In contrast to their $\delta^{13}C$ values, *P. variabilis* and *R. piscesae* displayed similar and relatively stable $\delta^{15}N$ values among samples with 0.3 ‰ (± 0.8 ‰) and 1.5 ‰ (± 1.1 ‰), respectively.

3.5. Biomass distribution in the Grotto trophic network

The projection of the species isotopic ratios weighted by biomass is useful for estimating the relative contributions of the different trophic pathways within the vent assemblages (Fig. 5). In our study, there were similar patterns of biomass distribution in the six sampled assemblages. In all samples, the engineer polychaete *R. piscesae* (species #1) represented the highest biomass (69.3 ± 16 %). It was considered to be a structuring species of our vent ecosystem and was not included in the following biomass distribution analysis. With a biomass ranging from 78.9 to 95.8 % (89.6 ± 6.8 %), gastropods seemed to play an important role in the trophic food web of communities associated with the siboglinid tubeworms. The gastropod biomass was dominated by *L. fucensis* (species #4), which accounted for 31.5 to 82.8 % (55.8 ± 18.3 %) of the total biomass. In addition to *L. fucensis*, the gastropods *D. globulus* (species #3), *P. variabilis* (species #2) and *Buccinum thermophilum* (species #5) showed relatively high biomass within the different samples, ranging from 5.6 to 36.6 % (16.5 ± 13.8 %), 0.6 to 26.3 % (10.9 ± 9.8 %) and 0 to 16.1 % (6.4 ± 6.8 %), respectively (Fig. 5). However, in some assemblages, other species also significantly contributed to the total biomass. For example, in S3, the polychaete *A. carldarei* (species #7) contributed substantially (7.2 %) to the total biomass. Similarly, in S4, the polychaete *P. palmiformis* (species #13) contributed to 16.4 % of the total biomass. Our results also show that the biomass declined from the bacterivore to the predator guilds in the Grotto trophic network.

4. Discussion

4.1. Communities and diversity

Hydrothermal ecosystems of the north-east Pacific are dominated by dense populations of tubeworms *R. piscesae*. In this study, a total of 36 macrofaunal taxonomic groups (including *R. piscesae*) were found in the six tubeworm assemblages sampled on the Grotto edifice, which is consistent with previous community knowledge in the region (Bergquist et al., 2007). In this study, macrofaunal species richness was slightly lower than that observed at the Easter Island hydrothermal site on the Main Endeavour Field, where a total of 39 species had been identified in a single *R. piscesae* bush (Bergquist et al., 2007). Another study also reported the presence of 39 macrofaunal species in 25 collections from the Axial Segment (JdFR), but lower values have been reported on other segments, with 24 species in 7 collections from the Cleft Segment (JdFR) and 19 species in 2 collections from the CoAxial Segment (JdFR) (Tsurumi and Tunnicliffe, 2003). These levels of diversity are lower than that found in *Riftia pachyptila* bushes on the East Pacific Rise, where species richness in 8 collections reached 46 taxa (Govenar et al., 2005). Macrofaunal diversity was also lower than those obtained in engineer mussel beds from Lucky Strike on the Mid-Atlantic Ridge, with 41 taxa identified (Sarrazin et al., 2015), or from the northern and southern East Pacific Rise, with richnesses of 61 and 57 taxa, respectively (Van Dover, 2003). Faunal dissimilarities between worldwide hydrothermal ecosystems may be closely related to the geological context (ridge, back-arc basins), history of species colonization, connectivity to neighbouring basins, presence of geographic barriers (transform faults, hydrodynamic processes, depths, etc.), stability of hydrothermal activity, age of the vent system and inter-site distances (Van Dover et al., 2002). Discrepancies in sampling effort may also account for variation between sites and regions.

R. piscesae tubeworm assemblages sampled on the Grotto edifice were characterized by the dominance of a few species (e.g. *L. fucensis*, *D. globulus*, *A. carldarei*), a pattern that has also been reported from other hydrothermal sites of the world oceans: Mid-Atlantic Ridge (Cuvelier et al., 2011; Sarrazin et al., 2015), East Pacific Rise (Govenar et al., 2005), JdFR (Sarrazin and Juniper, 1999; Tsurumi and Tunnicliffe, 2001) and the southern East Pacific Rise (Matabos et al., 2008). Polychaetes were the most diverse taxa, representing half of the

macrofaunal species richness (19 taxa). Similar results have been reported within *R. piscesae* bushes on Easter Island, with the identification of 23 polychaete species (Bergquist et al., 2007). Although the dominant species were similar among samples, variation between samples involved mainly the relative abundance of the few dominant species and the identity of the rare species. These variations may result from differences in sampling strategy. The areas sampled in 2016 were smaller than in 2015 and a problem with the sampling boxes may have led to the loss of some individuals. Variation in species richness and diversity among samples may also depend on the presence of environmental gradients, created by the mixing between ambient seawater and hydrothermal effluents (Sarrazin et al., 1999). Unfortunately, no environmental data were recorded with our samples. However, physical and chemical conditions are known to change along the ecological succession gradient on the MEF from newly opened habitat characterized by high temperature and sulfide concentrations, colonized by the sulfide worm *Paralvinella sulfincola*, to mature communities in low diffuse venting areas characterised by low temperatures and sulfide concentrations and colonized by long skinny *R. piscesae* tubeworms (Sarrazin et al., 1997). Tubeworm assemblages S1 and S3 were visually recognized as type V low-flow assemblages (Sarrazin et al., 1997), characterized by a mature phase of *R. piscesae* bush development and a high level of complexity. This assessment was confirmed by the length of the collected tubes (17 cm on average). Both assemblages showed the highest species richness, diversity and most complex trophic network, illustrating the strong influence of engineer species and the importance of biogenic structure in the diversification and persistence of the local resident fauna. By increasing the number of micro-niches available for vent species, the 3D structure of *R. piscesae* bushes helps to increase the environmental heterogeneity and thereby promotes species richness and diversity at community scales (Jones et al., 1997; Tsurumi and Tunnicliffe, 2003). As mentioned by several authors (Bergquist et al., 2003; Govenar et al., 2002; Tsurumi and Tunnicliffe, 2003), various ecological mechanisms may explain the influence of *R. piscesae* tubeworms on local diversity: new habitats generated by tubeworm bushes provide (*i*) a substratum for attachment and colonization; (*ii*) interstitial spaces among intertwined tubes, increasing habitat gradients and therefore the number of ecological niches; (*iii*) a refuge to avoid predators and to reduce the physiological stress related to abiotic conditions and (*iv*) a control on the transport of hydrothermal vent flow and nutritional resource availability. Assemblages S2 and S5, also identified as type V low-

flow assemblages (Sarrazin et al., 1997), presented shorter tube lengths than S1 and S3, which might explain the lower species richness in these two samples. Polychaete densities on Grotto were dominated by the ampharetid *A. carldarei* (89.9 ± 2.8 %, not including S4 and S6). High densities in *R. piscesae* assemblages may be related to the specificity of this family with high ecological tolerance to environmental conditions and, therefore, to their ability to take advantage of a wide range of ecological niches (McHugh and Tunnicliffe, 1994). Similar to *L. fucensis*, *A. carldarei* is characterized by early maturity and high fecundity, contributing to the success of this species in vent habitats (McHugh and Tunnicliffe, 1994). The dominance of gastropods *L. fucensis* and *D. globulus* as well as the relatively high presence of the *Paralvinella* polychaete species in samples S4 and S6 suggest that they belong to lower succession levels, corresponding to transitory states between types III and IV assemblages (Sarrazin et al., 1997). The latter two samples were characterized by low species richness and diversities. We hypothesize that the numerical dominance of gastropods negatively affected species diversity by monopolizing space and nutritional resources, therefore reducing the settlement of other vent species. The grazing of new recruits may also limit species diversity. Successional community dynamics leading to the development of tubeworm assemblages may thus result in the diversification of the habitats and of the species therein, and by a complexification of the trophic network, as suggested by Sarrazin *et al*. (2002) (Sarrazin et al., 2002).

4.2. Trophic structure of tubeworm assemblages

The *R. piscesae* tubeworm assemblages of the Grotto hydrothermal edifice harbour a relatively diverse heterotrophic fauna. The isotopic analyses conducted on the most dominant vent species within the bushes revealed a high degree of resemblance in trophic structure among the six faunal assemblages.

Hydrothermal food webs are generally based on two main energetic pathways: the transfer of energy from symbionts to host invertebrates and the consumption of free-living microbial production (Bergquist et al., 2007). In the present study, the contrasting isotope compositions of the gastropods *P. variabilis*, *L. fucensis* and the polychaete *R. piscesae* suggest three large pools of isotopically distinct, symbiotic and/or free-living microbial production available to primary consumers. The high $\delta^{13}C$ values of *R. piscesae* were

associated with chemosynthetic endosymbiosis linked to thiotrophic symbionts (Hügler and Sievert, 2011). *R. piscesae* contributed to 86 % of the assemblage biomass, but few species displayed similar $\delta^{13}C$ values, suggesting that species deriving their food sources from siboglinid tubeworms are rare. Similar observations, where engineer species contribute to the community more as a habitat than as a food source, have been reported in *R. piscesae* tubeworm bushes from the Easter Island vent site (Bergquist et al., 2007) or in *Bathymodiolus azoricus* mussel bed communities on the Tour Eiffel hydrothermal edifice (Lucky Strike, Mid-Atlantic Ridge) (De Busserolles et al., 2009). The low degree of exploitation of this large biomass and potential food resource suggests that *R. piscesae* plays a primarily structuring role in vent ecosystems rather than a trophic role. Nevertheless, the $\delta^{13}C$ and $\delta^{15}N$ values of polynoid predators *Branchinotogluma tunnicliffeae* and *Lepidonotopodium piscesae* were consistent with a diet including *R. piscesae* tubeworms. Predation on tubeworms was confirmed by a video sequence from the ecological observatory module TEMPO-mini, deployed on the Grotto hydrothermal edifice (ONC observatory; Video S1). The ^{13}C-depleted stable isotope compositions of *P. variabilis* suggest a possible symbiosis with chemoautotrophic bacteria or reliance on feeding on a very specific free-living microbial community that depends on a ^{13}C-depleted carbon source (Bergquist et al., 2007). To date, no study has reported the presence of chemoautotrophic symbionts in *P. variabilis*, but symbioses have been described for other species from the Provannidae family (Windoffer and Giere, 1997). With an intermediate $\delta^{13}C$ composition between *R. piscesae* and *P. variabilis*, *L. fucensis* gastropods seem to represent a major energetic pathway in these vent communities. In addition, the different food webs obtained in this study revealed that most vent species display an isotope composition centred on *L. fucensis*. The position of *L. fucensis* at the base of the food web probably reflects direct access to suspended food particles from hydrothermal fluid emissions. The high densities and large biomass of *L. fucensis* in tubeworm bushes, and its capacity to exploit different food sources through different feeding modes (Bates, 2007), may exert a high pressure on the availability of nutritional resources and, therefore, lead to an important role in structuring vent communities. Whenever present, the *Paralvinella* species, which are non-selective deposit-feeders, also displayed low $\delta^{15}N$ values, suggesting a role at the base of the food web. The stable isotope composition of *Paralvinella* species was much more variable

among samples than for the former three species, suggesting a possible variability in nutrient sources.

Like in many vent food webs (Van Dover and Fry, 1994; Levesque et al., 2005; Limén et al., 2007), Grotto primary consumers were dominated by grazers and deposit feeders. The high diversity, densities and biomass of bacterivores emphasize the importance of free-living bacteria in the establishment and maintenance of the structure of the vent food web (Bergquist et al., 2007). This guild was mainly represented by the gastropods *P. variabilis*, *D. globulus* and *L. fucensis* and by the polychaetes *P. sulfincola*, *P. palmiformis*, *P. pandorae* and *Paralvinella dela*. The polychaete *P. sulfincola* can feed directly on microbial biofilms on the substratum around its tube opening (Grelon et al., 2006), which may explain the low $\delta^{15}N$ values of alvinellids in the present study. Like *Paralvinella grasslei* and *Paralvinella bactericola* at vent sites of the Guaymas Basin (Portail et al., 2016), the alvinellid species found at Grotto had comparable $\delta^{13}C$ values but different $\delta^{15}N$ signatures. The species *P. pandorae* showed a depleted $\delta^{15}N$ signature relative to other alvinellid species. A previous study of spatial isotope variability among three sympatric alvinellid species, *P. palmiformis*, *P. sulfincola* and *P. pandorae* on the JdFR reported that this difference in $\delta^{15}N$ isotope composition was closely related to food-source partitioning and/or to spatial segregation (Levesque et al., 2003). The comparatively small size of *P. pandorae* (Lelièvre Y., personal observation) compared with other alvinellid species may be the result of interspecific competition for food resources and/or a diet based on an isotopically distinct microbial source. The wide range of $\delta^{13}C$ signatures in bacterivores, coupled with the high interspecific variability in the isotopic space, suggest a large, diversified microbial pool in the hydrothermal ecosystem and high variability in isotope ratios in dominant microbial taxa. Detritivore/scavenger species were observed at an intermediate trophic level, between the bacterivore and predator feeding guilds. This guild was represented by a low number of species including the gastropod *B. thermophilum*, the ampharetid *A. carldarei* and the orbiniid *Berkeleyia sp. nov*. The predator-feeding guild was represented by the highest $\delta^{15}N$ values. High predator diversity was found in our vent assemblages, and was associated with a wide range of $\delta^{13}C$ values, covering the isotopic spectrum of lower trophic level consumers (i.e. bacterivores as well as scavengers/detritivores). This guild of predators appears to be dominated by polychaetes, which tend to show the highest $\delta^{15}N$ values. Whenever present,

the syllid *Sphaerosyllis ridgensis*, the polynoid *Levensteiniella kincaidi* and the hesionid *Hesiospina sp. nov*. displayed the highest $\delta^{15}N$ values, suggesting that they play the role of top predators in the benthic food web. Similarly, the solenogaster *Helicoradomenia juani* consistently displayed higher $\delta^{15}N$ values than other molluscs, indicating a predator trophic position. Except for the polynoid *L. kincaidi*, whose isotopic variability seemed to reveal a nutrition based on highly diversified food resources, stable isotope analyses conducted on predators revealed narrow ranges of $\delta^{13}C$ and $\delta^{15}N$ values at the species scale, suggesting the dominance of specialist-feeding strategies, as was the case for the bacterivores. An accurate assessment of food sources and a description of the meiofaunal communities would be necessary to better understand the functioning of these chemosynthetic communities and their trophic structures.

4.3. Ecological niche partitioning

Vent species on the Grotto hydrothermal edifice exhibit high isotopic heterogeneity that reflects the complexity of vent ecological networks. The distribution of species in the bi-dimensional isotopic space depends on their diets, environmental conditions and biotic interactions, which together define the concept of species ecological niche (Newsome et al., 2007) or the realized species trophic niche (Bearhop et al., 2004). Here, the fact that most of the isotopic space was occupied by isotopically distinct species shows that the available food resources are partitioned within the community. Although the $\delta^{15}N$ variability among primary consumers did hinder our inference of trophic levels based on nitrogen isotopes, these communities are unlikely to host more than three trophic levels, given the overall $\delta^{15}N$ ranges. Moreover, although predators were quite diverse, they only represented a minor part of the biomass, suggesting that Grotto vent communities are mostly driven by bottom-up processes. Food webs of chemosynthetic ecosystems – such as hydrothermal vents and cold seeps – do not appear to be structured along predator-prey relationships, but rather through weak trophic relationships among co-occurring species (Levesque et al., 2006; Portail et al., 2016). Habitat and/or trophic partitioning are important structuring processes at the community scale (Levesque et al., 2003; Levin et al., 2013; Portail et al., 2016). Our results corroborate with those from Axial Volcano in the JdFR (Levesque et al., 2006) and the Guaymas basin (Portail et al., 2016), where habitat heterogeneity induces spatial partitioning of trophic niches, leading to a spatial segregation of species and species coexistence

554 (Levesque et al., 2006). Although the observed isotope variability (standard deviations) in
555 Grotto vent species suggests the occurrence of both trophic specialists and generalists
556 within the assemblages, the majority of vent species exhibited low standard deviations,
557 suggesting a predominantly specialist feeding behaviour. As already shown in previous
558 studies of vent sites with alvinellids (Levesque et al., 2003) and sulfidic sediments at
559 methane seeps with dorvilleid polychaetes (Levin et al., 2013) in the north-east Pacific, food
560 partitioning may occur between different species of the same or closely related taxonomic
561 family, allowing species coexistence through occupation of distinct trophic niches. For
562 example, hydrothermal vent gastropods were numerically dominant in all *R. piscesae* bushes
563 collected on the Grotto edifice and their isotope compositions were fairly diverse.
564 Gastropods exhibit great diversity in feeding strategies, and as a result they are found in a
565 wide variety of niches where they exploit many food sources (Bates et al., 2005; Bates,
566 2007). The isotope composition of *P. variabilis* indicated low $\delta^{13}C$ and $\delta^{15}N$ values. *L. fucensis*
567 gastropods had higher $\delta^{13}C$ and $\delta^{15}N$ values than *P. variabilis* but a similar range of $\delta^{13}C$ as
568 *Clypeosectus curvus* and *D. globulus*. However, these latter two species occupy an upper
569 position in the trophic structure of their communities. The great ecological success of *L.*
570 *fucensis* in vent habitats may be attributed to a combination of several characteristics. First,
571 this species is characterized by a broad trophic plasticity that includes: (*i*) grazing on
572 siboglinid tubeworms and hard substrata (Fretter, 1988), (*ii*) active suspension feeding
573 (Bates, 2007) and (*iii*) harbouring filamentous bacterial epibionts in its gills, which – via
574 endocytosis – may contribute to the animal's nutritional requirements (Bates, 2007; Fox et
575 al., 2002). In addition, the early maturity, high fecundity, and continuous gamete production
576 of *L. fucensis* may help to maintain the large populations on the edifice (Kelly and Metaxas,
577 2007). Stacking behaviour near fluid emissions also suggests that *L. fucensis* is an important
578 competitor for space and food in the community (Tsurumi and Tunnicliffe, 2003). *L. elevatus*,
579 the ecological equivalent of *L. fucensis* on the East Pacific Rise, is a prey for the vent zoarcid
580 fish *Thermarces cerberus*; the reduced limpet population promotes the successful
581 settlement and growth of sessile benthic invertebrates such as tubeworms (Micheli et al.,
582 2002; Sancho et al., 2005). The potential absence of an equivalent predator for *L. fucensis*
583 and the biological characteristics detailed above may explain its ecological success on the
584 north-east Pacific vent sites. In contrast, the nutrition of *D. globulus* is based on the grazing
585 of organic matter only (Warén and Bouchet, 1989). However, its small size allows it to

586 exploit interstitial spaces that are not available to larger fauna (Bates et al., 2005). Finally, *P.*
587 *variabilis* was relatively less abundant than the other two species, but appeared to exploit a
588 different thermal niche than *L. fucensis* and *D. globulus* (Bates et al., 2005). On the other
589 hand, the isotope composition of *B. thermophilum* clearly differentiates that species from
590 the other gastropods with higher $\delta^{13}C$ signatures. Differences in the diets of co-occurring
591 species may contribute to the high abundance – such as *L. fucensis* and *D. globulus* – and
592 diversity of vent gastropods through niche partitioning (Govenar et al., 2015).
593
594 Habitat specialization among co-occurring vent species may drive differences in their diets
595 (Govenar et al., 2015), facilitating species coexistence in heterogeneous habitats such as
596 hydrothermal ecosystems. We hypothesized that in vent engineering ecosystems, food webs
597 display a spatial structure at small scale with regard to the microhabitats generated by the
598 3D architecture of biogenic structures that promote high interspecific trophic segregation.
599 The spatial segregation of trophic niches by environmental gradients limits the occurrence of
600 biotic interactions such as predation and competition for resources between species sharing
601 a common spatial niche (Levesque et al., 2006). Vent food webs may therefore be structured
602 through the interplay between the availability and diversity of food sources and the abiotic
603 and biotic conditions structuring species distribution.
604

605 ## 5. Conclusion

606 This study provides the first characterization of the macrofaunal diversity and trophic
607 ecology of vent communities associated with *R. piscesae* tubeworm assemblages on the
608 Grotto hydrothermal edifice. Like many vent structures (Cuvelier et al., 2011; Sarrazin et al.,
609 1997), the Grotto hydrothermal edifice is inhabited by a mosaic of habitats and faunal
610 assemblages that may represent different successional stages characterized by different
611 abiotic conditions. Our results show that the development of *R. piscesae* tubeworms
612 introduces complexity and heterogeneity in the hydrothermal environments and exerts a
613 strong influence on ecosystem properties. The 3D structure of these tubeworms enhances
614 community diversity and thereby increases the potential trophic interactions between vent
615 species in the food web. Environmental gradients provided by the interstitial spacing of
616 intertwined tubeworms generate a multitude of ecological niches and contribute to the
617 partitioning of nutritional resources, leading to the species coexistence. Habitat

modifications incurred by *R. piscesae* bushes may thus directly stimulate the development of complex food webs. Thorough knowledge of hydrothermal biodiversity and ecological functioning of these remote ecosystems is necessary to determine their uniqueness and contribute to the protection and conservation of this natural heritage.

Author's contributions

M.M., J.S. and P.L. designed and supervised the research project. Y.L., J.M., T.D. and S.H.: data acquisition and analyses. Y.L., M.M., J.S., G.S. and P.L. conceived the ideas and contributed to the interpretation of the results. All authors contributed to the writing process and revised the manuscript.

Competing interests

The authors declare that they have no conflict of interest.

Acknowledgments

The authors thank the captains and crews of the R/V *Thomas G. Thompson* and E/V *Nautilus*, the staffs of Ocean Networks Canada and ROV *Jason* and *Hercules* pilots during the "*Ocean Networks Canada Wiring the Abyss*" cruises in 2015 and 2016. We thank also Kim Juniper and the government of Canada for work permits to study in Canadian waters (XR281, 2015; XR267, 2016). Thanks also to Pauline Chauvet for faunal sampling during the ONC 2016 cruise. This research was supported by a NSERC research grant to P.L. and IFREMER funds. It was also funded by the *Laboratoire d'Excellence* LabexMER (ANR-10-LABX-19) and co-funded by a grant from the French government under the *Investissements d'Avenir* programme. We are also grateful to the numerous taxonomists around the world who contributed to species identification and to the laboratory *Centre de Recherche sur les Interactions Bassins Versants - Écosystèmes Aquatiques* (RIVE) at the Université du Québec à Trois-Rivières (Canada) for the isotope sample processing. The manuscript was professionally edited by Carolyn Engel-Gautier. This paper is part of the Ph.D. thesis of Y.L. carried out under joint supervision between Université de Montréal and Université de Bretagne Occidentale/Ifremer.

References

Bachraty, C., Legendre, P. and Desbruyères, D.: Biogeographic relationships among deep-sea hydrothermal vent faunas at global scale, Deep. Res. Part I Oceanogr. Res. Pap., 56(8), 1371–1378, 2009.

Bates, A., Tunnicliffe, V. and Lee, R. W.: Role of thermal conditions in habitat selection by hydrothermal vent gastropods, Mar. Ecol. Prog. Ser., 305, 1–15, 2005.

Bates, A. E.: Feeding strategy, morphological specialisation and presence of bacterial episymbionts in lepetodrilid gastropods from hydrothermal vents, Mar. Ecol. Prog. Ser., 347, 87–99, 2007.

Bearhop, S., Adams, C. E., Waldron, S., Fuller, R. A. and Macleod, H.: Determining trophic niche width: a novel approach using stable isotope analysis, J. Anim. Ecol., 73(5), 1007–1012, 2004.

Bergquist, D., Ward, T., Cordes, E., McNelis, T., Howlett, S., Kosoff, R., Hourdez, S., Carney, R. and Fisher, C.: Community structure of vestimentiferan-generated habitat islands from Gulf of Mexico cold seeps, J. Exp. Mar. Bio. Ecol., 289(2), 197–222, 2003.

Bergquist, D. C., Eckner, J. T., Urcuyo, I. A., Cordes, E. E., Hourdez, S., Macko, S. A. and Fisher, C. R.: Using stable isotopes and quantitative community characteristics to determine a local hydrothermal vent food web, Mar. Ecol. Prog. Ser., 330(1), 49–65, 2007.

De Busserolles, F., Sarrazin, J., Gauthier, O., Gélinas, Y., Fabri, M.-C., Sarradin, P.-M. and Desbruyères, D.: Are spatial variations in the diets of hydrothermal fauna linked to local environmental conditions?, Deep. Res. Part II Top. Stud. Oceanogr., 56(19–20), 1649–1664, 2009.

Childress, J. J. and Fisher, C. R.: The biology of hydrothermal vent animals: physiology, biochemistry, and autotrophic symbioses, Oceanogr. Mar. Biol. Annu. Rev., 30, 337–441, 1992.

Conway, N. M., Kennicutt, M. C. and Van Dover, C. L.: Stable isotopes in the study of marine chemosynthetic-based ecosystems, in Stable isotopes in ecology and environmental science, pp. 158–186., 1994.

Cuvelier, D., Sarradin, P.-M., Sarrazin, J., Colaço, A., Copley, J. T., Desbruyères, D., Glover, A. G., Serrao Santos, R. and Tyler, P. A.: Hydrothermal faunal assemblages and habitat characterisation at the Eiffel Tower edifice (Lucky Strike, Mid-Atlantic Ridge), Mar. Ecol.,

679 32(2), 243–255, 2011.
680 Cuvelier, D., De Busserolles, F., Lavaud, R., Floc'h, E., Fabri, M.-C., Sarradin, P. M. and
681 Sarrazin, J.: Biological data extraction from imagery - How far can we go? A case study from
682 the Mid-Atlantic Ridge, Mar. Environ. Res., 82, 15–27, 2012.
683 Cuvelier, D., Legendre, P., Laes, A., Sarradin, P.-M. and Sarrazin, J.: Rhythms and community
684 dynamics of a hydrothermal tubeworm assemblage at Main Endeavour Field - A
685 multidisciplinary deep-sea observatory approach, PLoS One, 9(5), e96924, 2014.
686 Delaney, J. R., Robigou, V., McDuff, R. E. and Tivey, M. K.: Geology of a vigorous
687 hydrothermal system on the Endeavour Segment, Juan de Fuca Ridge, J. Geophys. Res.,
688 97(B13), 19663–19682, 1992.
689 Van Dover, C. L.: Trophic relationships among invertebrates at the Kairei hydrothermal vent
690 field (Central Indian Ridge), Mar. Biol., 141(4), 761–772, 2002.
691 Van Dover, C. L.: Variation in community structure within hydothermal vent mussel beds of
692 the East Pacific Rise, Mar. Ecol. Prog. Ser., 253, 55–66, 2003.
693 Van Dover, C. L. and Fry, B.: Stable isotopic compositions of hydrothermal vent organisms,
694 Mar. Biol., 102(2), 257–263, 1989.
695 Van Dover, C. L. and Trask, J. L.: Diversity at deep-sea hydrothermal vent and intertidal
696 mussel beds, Mar. Ecol. Prog. Ser., 195, 169–178, 2000.
697 Van Dover, C. L., German, C. R., Speer, K. G., Parson, L. M. and Vrijenhoek, R. C.: Evolution
698 and biogeography of deep-sea vent and seep invertebrates, Science., 295(5558), 1253–1257,
699 doi:10.1126/science.1067361, 2002.
700 Van Dover, C. and Fry, B.: Microorganisms as food resources at deep-sea hydrothermal
701 vents, Limnol. Oceanogr., 39(1), 51–57, 1994.
702 Dreyer, J. C., Knick, K. E., Flickinger, W. B. and Van Dover, C. L.: Development of macrofaunal
703 community structure in mussel beds on the northern East Pacific Rise, Mar. Ecol. Prog. Ser.,
704 302, 121–134, 2005.
705 Erickson, K. L., Macko, S. A. and Van Dover, C. L.: Evidence for a chemoautotrophically based
706 food web at inactive hydrothermal vents (Manus Basin), Deep. Res. Part II Top. Stud.
707 Oceanogr., 56(19–20), 1577–1585, 2009.
708 Fisher, C., Takai, K. and Le Bris, N.: Hydrothermal vent ecosystems, Oceanography, 20(1), 14–
709 23, 2007.
710 Fox, M., Juniper, S. K. and Vali, H.: Chemoautotrophy as a possible nutritional source in the

711 hydrothermal vent limpet *Lepetodrilus fucensis*, Cah. Biol. Mar., 43, 371–376, 2002.
712 Fretter, V.: New archaeogastropod limpets from hydrothermal vents ; supermfamily
713 Lepetodrilacea, Philos. Trans. R. Soc. London, 318, 33–82, 1988.
714 Galkin, S. V. and Goroslavskaya, E. I.: Bottom fauna associated with *Bathymodiolus azoricus*
715 (Mytilidae) mussel beds in the hydrothermal fields of the Mid-Atlantic Ridge, Oceanology,
716 50(1), 51–60, 2010.
717 Gaudron, S. M., Lefebvre, S., Nunes Jorge, A., Gaill, F. and Pradillon, F.: Spatial and temporal
718 variations in food web structure from newly-opened habitat at hydrothermal vents, Mar.
719 Environ. Res., 77, 129–140, 2012.
720 Gollner, S., Zekely, J., Dover, C. L. Van, Govenar, B., Le Bris, N., Nemeschkal, H. L., Bright, M.,
721 Hole, W. and Hole, W.: Benthic copepod communities associated with tubeworm and mussel
722 aggregations on the East Pacific Rise, Cah. Biol. Mar., 47(4), 397–402, 2006.
723 Govenar, B. and Fisher, C. R.: Experimental evidence of habitat provision by aggregations of
724 *Riftia pachyptila* at hydrothermal vents on the East Pacific Rise, Mar. Ecol., 28(1), 3–14,
725 2007.
726 Govenar, B., Le Bris, N., Gollner, S., Glanville, J., Aperghis, A. B., Hourdez, S. and Fisher, C. R.:
727 Epifaunal community structure associated with *Riftia pachyptila* aggregations in chemically
728 different hydrothermal vent habitats, Mar. Ecol. Prog. Ser., 305, 67–77, 2005.
729 Govenar, B., Fisher, C. R. and Shank, T. M.: Variation in the diets of hydrothermal vent
730 gastropods, Deep. Res. Part II Top. Stud. Oceanogr., 121, 193–201, 2015.
731 Govenar, B. W., Bergquist, D. C., Urcuyo, I. A., Eckner, J. T. and Fisher, C. R.: Three Ridgeia
732 piscesae assemblages from a single Juan de Fuca Ridge sulphide edifice: Structurally
733 different and functionally similar, Cah. Biol. Mar., 43(3–4), 247–252, 2002.
734 Gray, J. S.: The measurement of marine species diversity, with an application to the benthic
735 fauna of the Norwegian continental shelf., J. Exp. Mar. Bio. Ecol., 250(1), 23–49, 2000.
736 Grelon, D., Morineaux, M., Desrosiers, G. and Juniper, K.: Feeding and territorial behavior of
737 *Paralvinella sulfincola*, a polychaete worm at deep-sea hydrothermal vents of the Northeast
738 Pacific Ocean, J. Exp. Mar. Bio. Ecol., 329(2), 174–186, 2006.
739 Hügler, M. and Sievert, S. M.: Beyond the Calvin cycle: autotrophic carbon fixation in the
740 ocean, Ann. Rev. Mar. Sci., 3, 261–289, 2011.
741 Jones, C. G., Lawton, J. H. and Shachak, M.: Organisms as ecosystem engineers, in Ecosystem
742 management, vol. 69, edited by Springer New York, pp. 130–147., 1994.

743 Jones, C. G., Lawton, J. H. and Shachak, M.: Positive and negative effects of organisms as
744 physical ecosystem engineers, , 78(7), 1946–1957, 1997.
745 Juniper, S. K., Jonasson, I. R., Tunnicliffe, V. and Southward, A. J.: Influence of a tube-building
746 polychaete on hydrothermal chimney mineralization, Geology, 20(10), 895–898, 1992.
747 Kelley, D. S., Carbotte, S. M., Caress, D. W., Clague, D. A., Delaney, J. R., Gill, J. B., Hadaway,
748 H., Holden, J. F., Hooft, E. E. E., Kellogg, J. P., Lilley, M. D., Stoermer, M., Toomey, D., Weekly,
749 R. and Wilcock, W. S. D.: Endeavour Segment of the Juan de Fuca Ridge: one of the most
750 remarkable places on earth, Oceanography, 25(1), 44–61, 2012.
751 Kelly, N. E. and Metaxas, A.: Influence of habitat on the reproductive biology of the deep-sea
752 hydrothermal vent limpet *Lepetodrilus fucensis* (Vetigastropoda: Mollusca) from the
753 Northeast Pacific, Mar. Biol., 151(2), 649–662, 2007.
754 Lelièvre, Y., Legendre, P., Matabos, M., Mihály, S., Lee, R. W., Sarradin, P.-M., Arango, C. P.
755 and Sarrazin, J.: Astronomical and atmospheric impacts on deep-sea hydrothermal vent
756 invertebrates, Proc. R. Soc. B Biol. Sci., 284(1852), 20162123, 2017.
757 Lenihan, H. S., Mills, S. W., Mullineaux, L. S., Peterson, C. H., Fisher, C. R. and Micheli, F.:
758 Biotic interactions at hydrothermal vents: Recruitment inhibition by the mussel
759 *Bathymodiolus thermophilus*, Deep. Res. Part I Oceanogr. Res. Pap., 55(12), 1707–1717,
760 2008.
761 Levesque, C., Juniper, S. K. and Marcus, J.: Food resource partitioning and competition
762 among alvinellid polychaetes of Juan de Fuca Ridge hydrothermal vents, Mar. Ecol. Prog.
763 Ser., 246, 173–182, 2003.
764 Levesque, C., Limén, H. and Juniper, S. K.: Origin, composition and nutritional quality of
765 particulate matter at deep-sea hydrothermal vents on Axial Volcano, NE Pacific, Mar. Ecol.
766 Prog. Ser., 289, 43–52, 2005.
767 Levesque, C., Kim Juniper, S. and Limén, H.: Spatial organization of food webs along habitat
768 gradients at deep-sea hydrothermal vents on Axial Volcano, Northeast Pacific, Deep. Res.
769 Part I Oceanogr. Res. Pap., 53(4), 726–739, 2006.
770 Levin, L. A. and Michener, R. H.: Isotopic evidence for chemosynthesis-based nutrition of
771 macrobenthos: the lightness of being at Pacific methane seeps, Limnol. Oceanogr., 47(5),
772 1336–1345, 2002.
773 Levin, L. A., Mendoza, G. F., Konotchick, T. and Lee, R.: Macrobenthos community structure
774 and trophic relationships within active and inactive Pacific hydrothermal sediments, Deep.

Res. Part II Top. Stud. Oceanogr., 56(19–20), 1632–1648, 2009.
Levin, L. A., Ziebis, W., F. Mendoza, G., Bertics, V. J., Washington, T., Gonzalez, J., Thurber, A. R., Ebbe, B. and Lee, R. W.: Ecological release and niche partitioning under stress: Lessons from dorvilleid polychaetes in sulfidic sediments at methane seeps, Deep. Res. Part II Top. Stud. Oceanogr., 92, 214–233, 2013.
Limén, H., Levesque, C. and Kim Juniper, S.: POM in macro-/meiofaunal food webs associated with three flow regimes at deep-sea hydrothermal vents on Axial Volcano, Juan de Fuca Ridge, Mar. Biol., 153(2), 129–139, 2007.
Luther, G., Rozan, T., Taillefert, M., Nuzzio, D., Di Meo, C., Shank, T., Lutz, R. and Cary, C.: Chemical speciation drives hydrothermal vent ecology., Nature, 410(6830), 813–816, 2001.
Marcus, J., Tunnicliffe, V. and Butterfield, D. A.: Post-eruption succession of macrofaunal communities at diffuse flow hydrothermal vents on Axial Volcano, Juan de Fuca Ridge, Northeast Pacific, Deep. Res. Part II Top. Stud. Oceanogr., 56(19–20), 1586–1598, 2009.
Matabos, M., Le Bris, N., Pendlebury, S. and Thiebaut, E.: Role of physico-chemical environment on gastropod assemblages at hydrothermal vents on the East Pacific Rise (13 degrees N/EPR), J. Mar. Biol. Assoc. United Kingdom, 88(5), 995–1008, 2008.
Matabos, M., Cuvelier, D., Brouard, J., Shillito, B., Ravaux, J., Zbinden, M., Barthelemy, D., Sarradin, P.-M. and Sarrazin, J.: Behavioural study of two hydrothermal crustacean decapods: Mirocaris fortunata and Segonzacia mesatlantica, from the lucky strike vent field (mid-Atlantic Ridge), Deep Sea Res. Part II Top. Stud. Oceanogr., 121, 146–158 [online] Available from: http://linkinghub.elsevier.com/retrieve/pii/S0967064515001113, 2015.
McHugh, D. and Tunnicliffe, V.: Ecology and reproductive biology of the hydrothermal vent polychaete *Amphisamytha galapagensis* (Ampharetidae), Mar. Ecol. Prog. Ser., 106, 111–120, 1994.
Micheli, F., Peterson, C. H., Mullineaux, L. S., Fisher, C. R., Mills, S. W., Sancho, G., Johnson, G. a. and Lenihan, H. S.: Predation structures communities at deep-sea hydrothermal vents, Ecol. Monogr., 72(3), 365–382, 2002.
Michener, R. and Lajtha, K.: Stable isotopes in ecology and environmental science, Blackwell., 2008.
Moalic, Y., Desbruyères, D., Duarte, C. M., Rozenfeld, A. F., Bachraty, C. and Arnaud-Haond, S.: Biogeography revisited with network theory: Retracing the history of hydrothermal vent communities, Syst. Biol., 61(1), 127–137, 2011.

807 Mullineaux, L. S., Fisher, C. R., Peterson, C. H. and Schaeffer, S. W.: Tubeworm succession at
808 hydrothermal vents: use of biogenic cues to reduce habitat selection error?, Oecologia,
809 123(2), 275–284, 2000.
810 Mullineaux, L. S., Peterson, C. H., Micheli, F. and Mills, S. W.: Successional mechanism varies
811 along a gradient in hydrothermal fluid flux at deep-sea vents, Ecol. Monogr., 73(4), 523–542,
812 2003.
813 Nedoncelle, K., Lartaud, F., de Rafelis, M., Boulila, S. and Le Bris, N.: A new method for high-
814 resolution bivalve growth rate studies in hydrothermal environments, Mar. Biol., 160(6),
815 1427–1439, 2013.
816 Nedoncelle, K., Lartaud, F., Contreira-Pereira, L., Yücel, M., Thurnherr, A. M., Mullineaux, L.
817 and Le Bris, N.: *Bathymodiolus* growth dynamics in relation to environmental fluctuations in
818 vent habitats, Deep Sea Res. Part I Oceanogr. Res. Pap., 106, 183–193, 2015.
819 Newsome, S. D., del Rio, C. M., Bearhop, S. and Phillips, D. L.: A niche for isotopic ecology,
820 Front. Ecol. Environ., 5(8), 429–436, 2007.
821 Oksanen, J., Blanchet, F. G., Friendly, M., Kindt, R., Legendre, P., Mcglinn, D., Minchin, P. R.,
822 O'hara, R. B., Simpson, G. L., Solymos, P., Henry, M., Stevens, H., Szoecs, E. and Wagner, H.:
823 vegan: Community Ecology Package, R Packag. version 2.4-2, https://CRAN.R-
824 project.org/package=vegan, 2017.
825 Portail, M., Olu, K., Dubois, S. F., Escobar-Briones, E., Gelinas, Y., Menot, L. and Sarrazin, J.:
826 Food-web complexity in Guaymas Basin hydrothermal vents and cold seeps, PLoS One, 11(9),
827 e0162263, 2016.
828 Ramirez-Llodra, E., Shank, T. and German, C.: Biodiversity and biogeography of hydrothermal
829 vent species: thirty years of discovery and investigations, Oceanography, 20(1), 30–41, 2007.
830 Sancho, G., Fisher, C. R., Mills, S., Micheli, F., Johnson, G. a., Lenihan, H. S., Peterson, C. H.
831 and Mullineaux, L. S.: Selective predation by the zoarcid fish *Thermarces cerberus* at
832 hydrothermal vents, Deep. Res. Part I Oceanogr. Res. Pap., 52(5), 837–844, 2005.
833 Sarrazin, J. and Juniper, S. K.: Biological characteristics of a hydrothermal edifice mosaic
834 community, Mar. Ecol. Prog. Ser., 185, 1–19, 1999.
835 Sarrazin, J., Robigou, V., Juniper, S. K. and Delaney, J. R.: Biological and geological dynamics
836 over four years on a high-temperature sulfide structure at the Juan de Fuca Ridge
837 hydrothermal observatory, Mar. Ecol. Prog. Ser., 153(1–3), 5–24, 1997.
838 Sarrazin, J., Juniper, S. K., Massoth, G. and Legendre, P.: Physical and chemical factors

influencing species distributions on hydrothermal sulfide edifices of the Juan de Fuca Ridge, northeast Pacific, Mar. Ecol. Prog. Ser., 190, 89–112, 1999.

Sarrazin, J., Levesque, C., Juniper, S. K. and Tivey, M. K.: Mosaic community dynamics on Juan de Fuca Ridge sulphide edifices: Substratum, temperature and implications for trophic structure, Cah. Biol. Mar., 43(3–4), 275–279, 2002.

Sarrazin, J., Cuvelier, D., Peton, L., Legendre, P. and Sarradin, P.-M.: High-resolution dynamics of a deep-sea hydrothermal mussel assemblage monitored by the EMSO-Açores MoMAR observatory, Deep. Res. Part I Oceanogr. Res. Pap., 90(1), 62–75, 2014.

Sarrazin, J., Legendre, P., de Busserolles, F., Fabri, M. C., Guilini, K., Ivanenko, V. N., Morineaux, M., Vanreusel, A. and Sarradin, P. M.: Biodiversity patterns, environmental drivers and indicator species on a high-temperature hydrothermal edifice, Mid-Atlantic Ridge, Deep. Res. Part II Top. Stud. Oceanogr., 121, 177–192, 2015.

Soto, L. A.: Stable carbon and nitrogen isotopic signatures of fauna associated with the deep-sea hydrothermal vent system of Guaymas Basin, Gulf of California, Deep Sea Res. Part II Top. Stud. Oceanogr., 56(19–20), 1675–1682, 2009.

Sweetman, A. K., Levin, L. A., Rapp, H. T. and Schander, C.: Faunal trophic structure at hydrothermal vents on the southern Mohn's Ridge, Arctic Ocean, Mar. Ecol. Prog. Ser., 473, 115–131, 2013.

Tsurumi, M. and Tunnicliffe, V.: Characteristics of a hydrothermal vent assemblage on a volcanically active segment of Juan de Fuca Ridge, northeast Pacific, Can. J. Fish. Aquat. Sci., 58(3), 530–542, 2001.

Tsurumi, M. and Tunnicliffe, V.: Tubeworm-associated communities at hydrothermal vents on the Juan de Fuca Ridge, northeast Pacific, Deep. Res. Part I Oceanogr. Res. Pap., 50(5), 611–629, 2003.

Tunnicliffe, V.: The biology of hydrothermal vents: ecology and evolution, Oceanogr. Mar. Biol. Annu. Rev., 29, 319–407, 1991.

Turnipseed, M., Knick, K. E., Lipcius, R. N., Dreyer, J. and Van Dover, C. L.: Diversity in mussel beds at deep-sea hydrothermal vents and cold seeps, Ecol. Lett., 6, 518–523, 2003.

Urcuyo, I., Massoth, G., Julian, D. and Fisher, C.: Habitat, growth and physiological ecology of a basaltic community of *Ridgeia piscesae* from the Juan de Fuca Ridge, Deep. Res. Part I Oceanogr. Res. Pap., 50(6), 763–780, 2003.

Warén, A. and Bouchet, P.: New gastropods from East Pacific hydrothermal vents, Zool. Scr.,

18(1), 67–102, 1989.
Windoffer, R. and Giere, O.: Symbiosis of the hydrothermal vent gastropod *Ifremeria nautilei* (Provannidae) with endobacteria-structural analyses and ecological considerations, Biol. Bull., 193(3), 381–392, 1997.
Xu, G., Jackson, D. R., Bemis, K. G. and Rona, P. A.: Time-series measurement of hydrothermal heat flux at the Grotto mound, Endeavour Segment, Juan de Fuca Ridge, Earth Planet. Sci. Lett., 404, 220–231, 2014.
Zekely, J., Van Dover, C. L., Nemeschkal, H. L. and Bright, M.: Hydrothermal vent meiobenthos associated with mytilid mussel aggregations from the Mid-Atlantic Ridge and the East Pacific Rise, Deep. Res. Part I Oceanogr. Res. Pap., 53, 1363–1378, 2006.

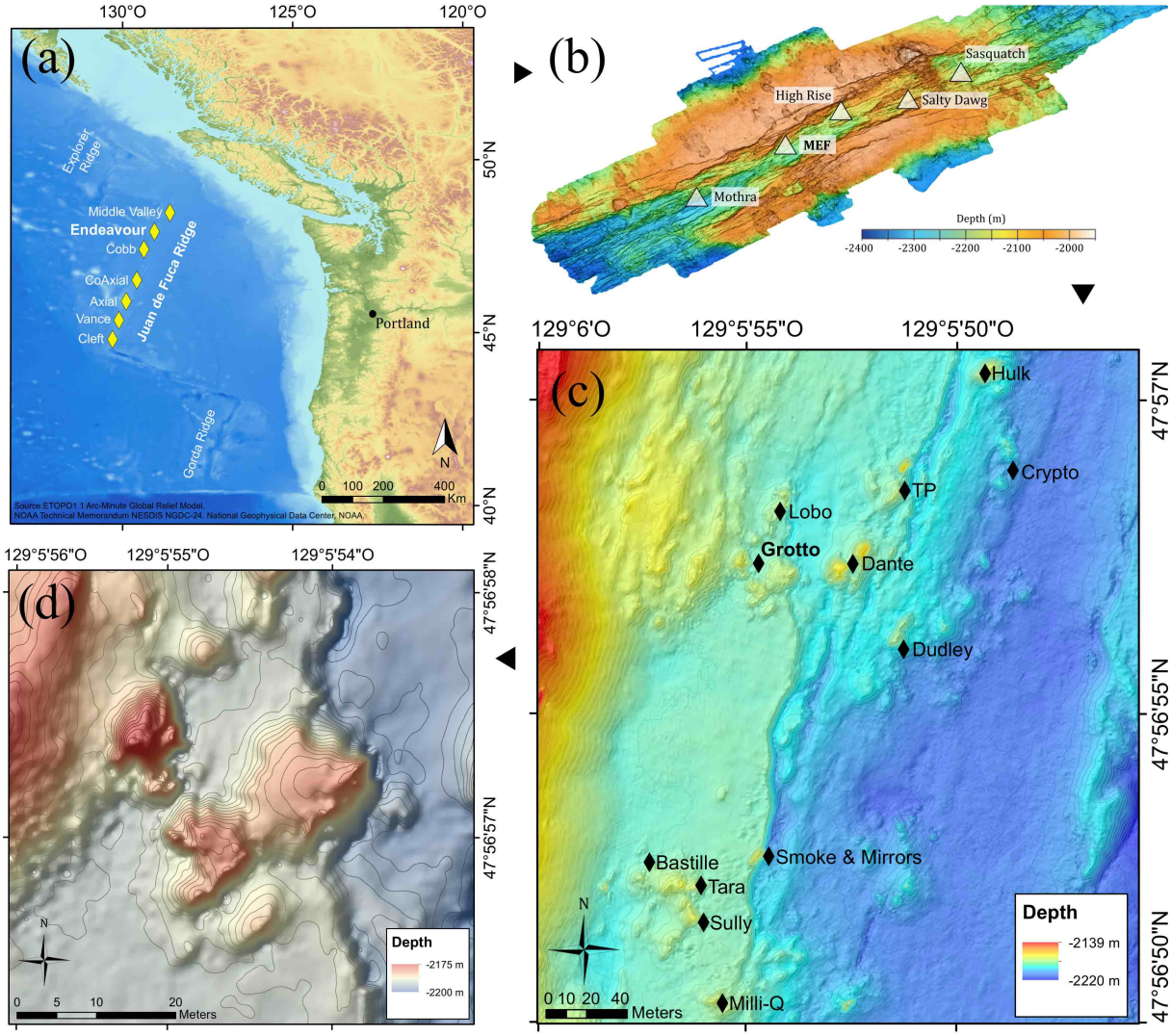

Figure 1. (a) Location of the Juan de Fuca Ridge system and the seven segments (yellow diamonds). (b) High-resolution bathymetric map of the Endeavour Segment, with the locations of the five main active vent fields (white triangle). (c) Location map of the Main Endeavour vent field indicating the positions of hydrothermal vent edifices (black diamonds). (d) Bathymetric map of the Grotto active hydrothermal edifice (47°56.958'N, 129°5.899'W). The 10 m high sulfide structure is located in the Main Endeavour vent field.

903
904
905
906
907
908

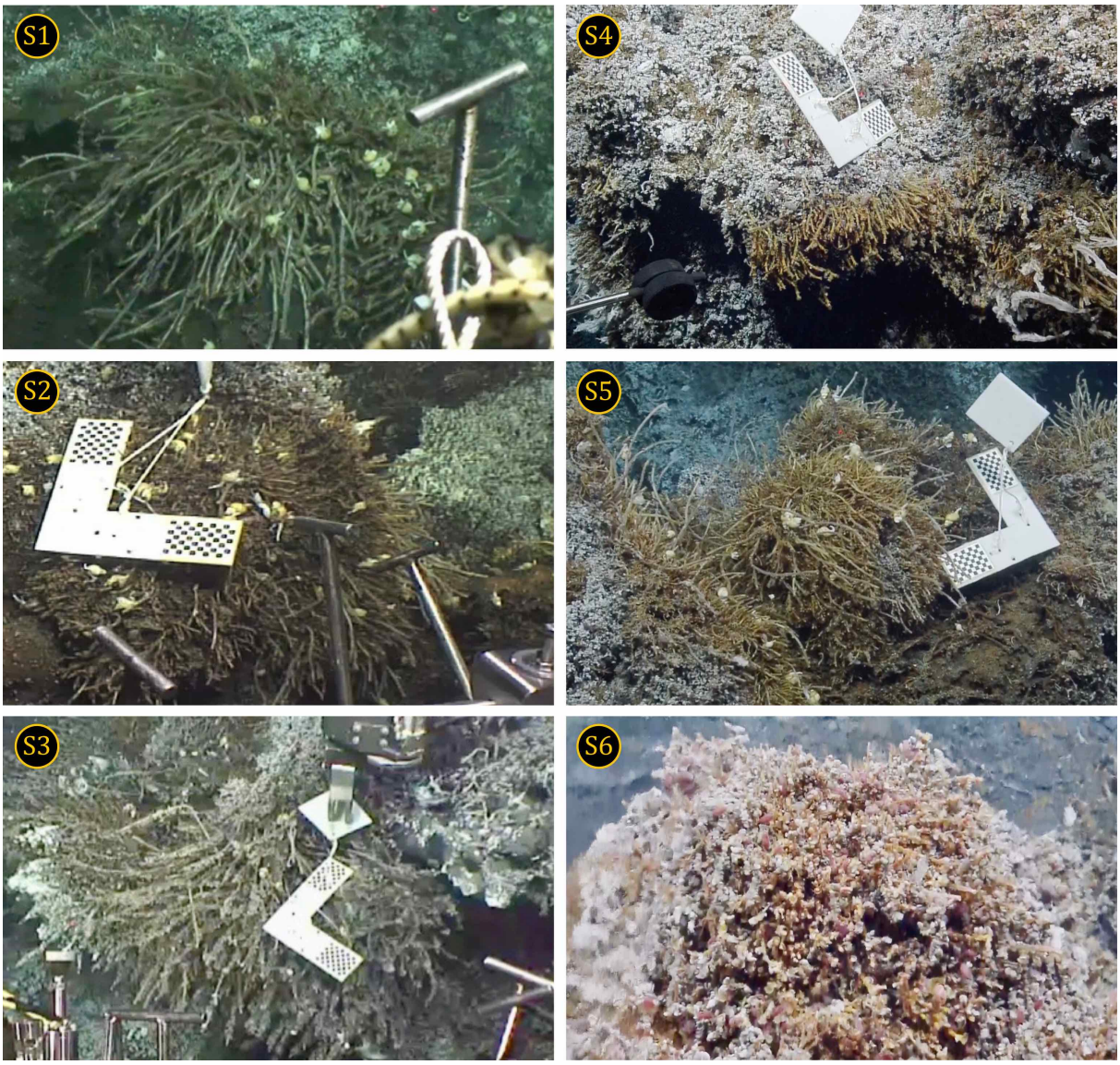

Figure 2. Hydrothermal communities collected on the Grotto edifice (Main Endeavour, Juan de Fuca Ridge) during *Ocean Networks Canada* oceanographic cruises *Wiring the Abyss 2015 and 2016*.

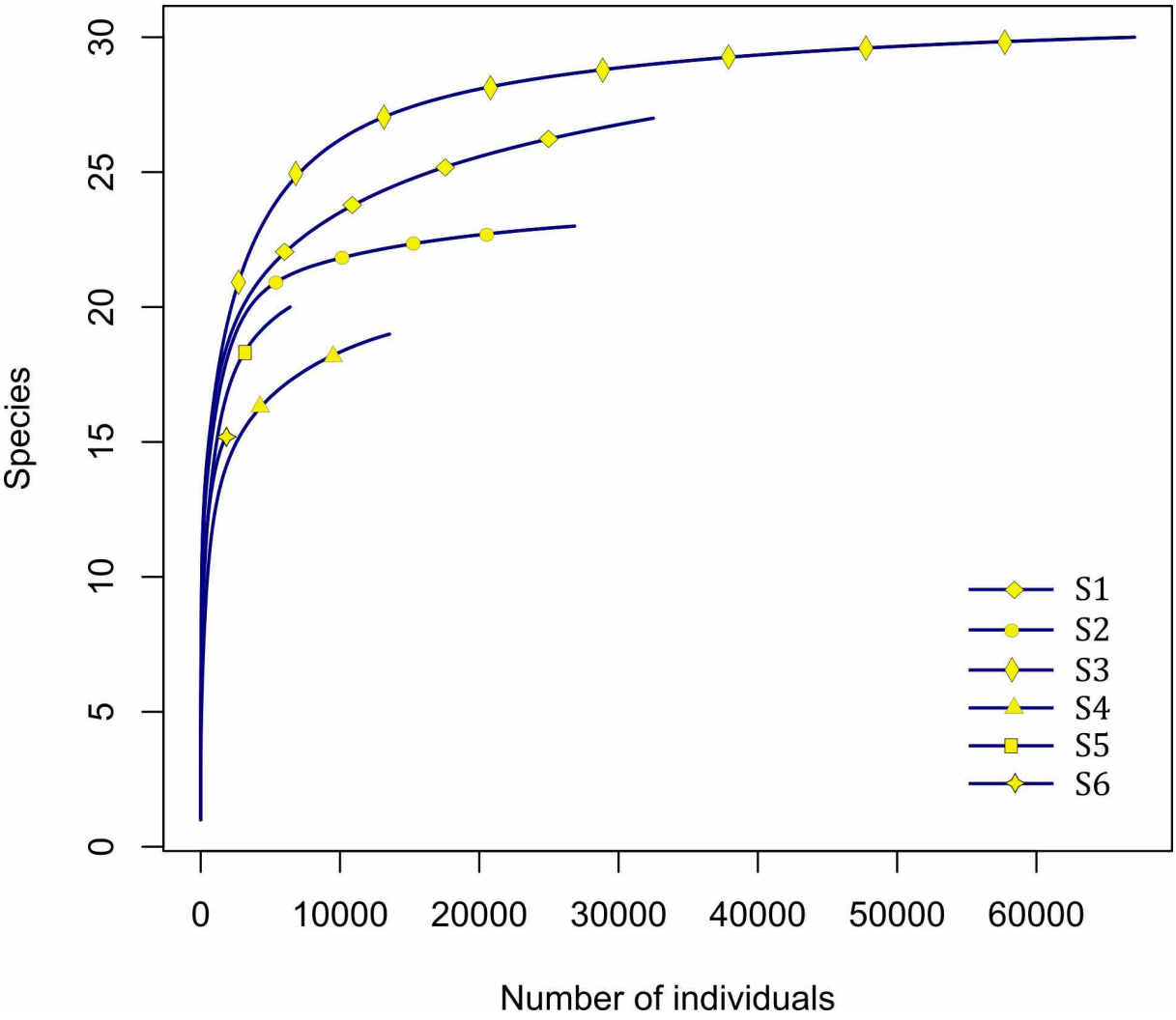

Figure 3. Rarefaction curves for species richness in six vent assemblages (S1 to S6) sampled on the Grotto hydrothermal edifice.

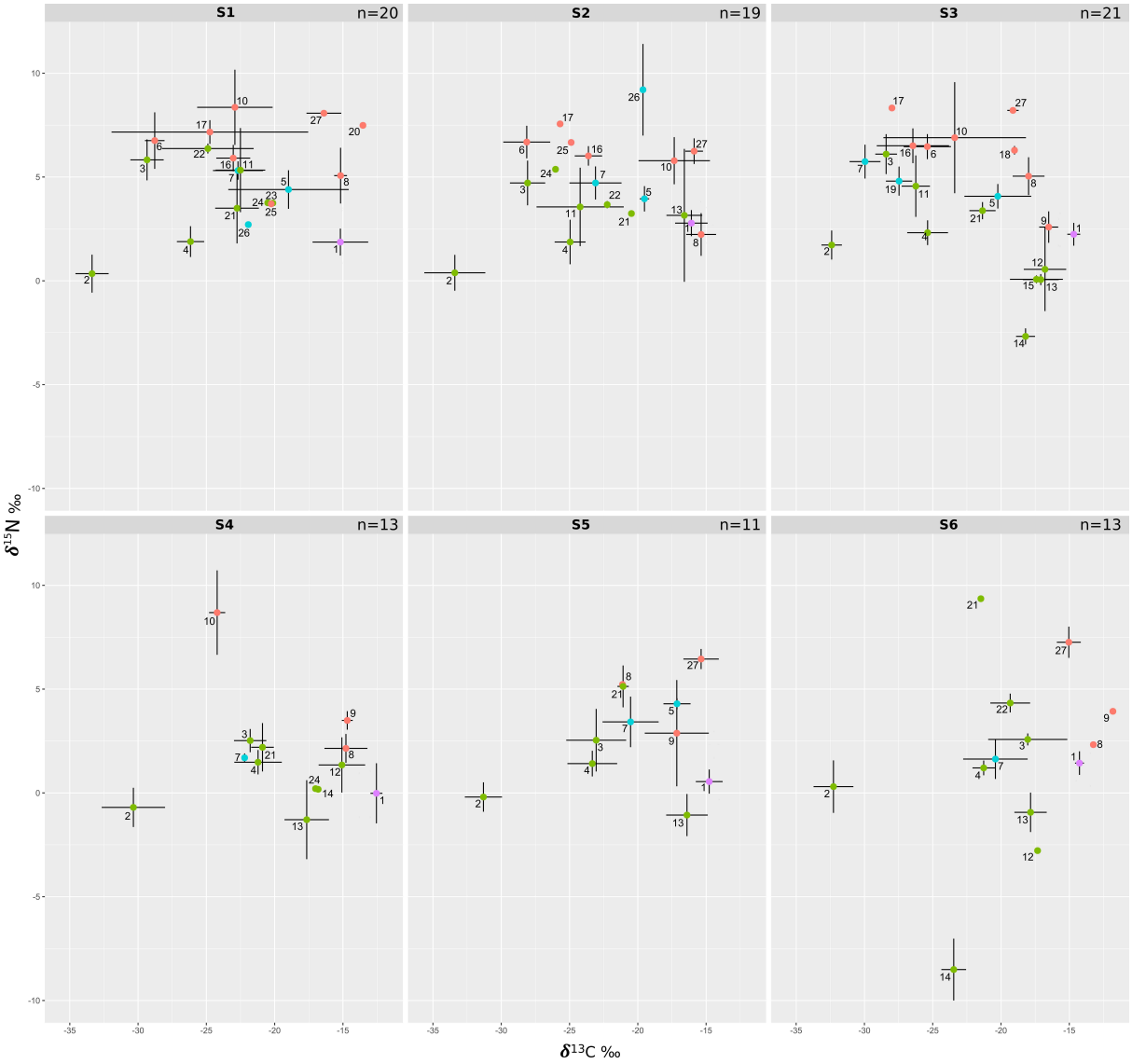

Figure 4. Stable isotope bi-plots showing vent consumers' isotope signatures (mean $\delta^{13}C$ versus $\delta^{15}N$ values ± standard deviation) for the six vent assemblages sampled on the Grotto hydrothermal edifice. Each vent species is designated by a number: 1 = *Ridgeia piscesae*; 2 = *Provanna variabilis*; 3 = *Depressigyra globulus*; 4 = *Lepetodrilus fucensis*; 5 = *Buccinum thermophilum*; 6 = *Clypeosectus curvus*; 7 = *Amphisamytha carldarei*; 8 = *Branchinotogluma tunnicliffeae*; 9 = *Lepidonotopodium piscesae*; 10 = *Levensteiniella kincaidi*; 11 = *Nicomache venticola*; 12 = *Paralvinella sulfincola*; 13 = *Paralvinella palmiformis*; 14 = *Paralvinella pandorae*; 15 = *Paralvinella dela*; 16 = *Hesiospina sp. nov.*; 17 = *Sphaerosyllis ridgensis*; 18 = *Ophryotrocha globopalpata*; 19 = *Berkeleyia sp. nov.*; 20 = *Protomystides verenae*; 21 = *Sericosura* sp.; 22 = *Euphilomedes climax*; 23 = *Xylocythere sp. nov.*; 24 = Copepoda; 25 = *Copidognathus papillatus*; 26 = *Paralicella vaporalis*; 27 = *Helicoradomenia juani*. Known trophic guilds are distinguished by a colour code: pink: symbiont; green: bacterivores; blue: scavengers/detritivores; red: predators. For more information on the interpretation of guilds, please consult the web version of this paper.

929

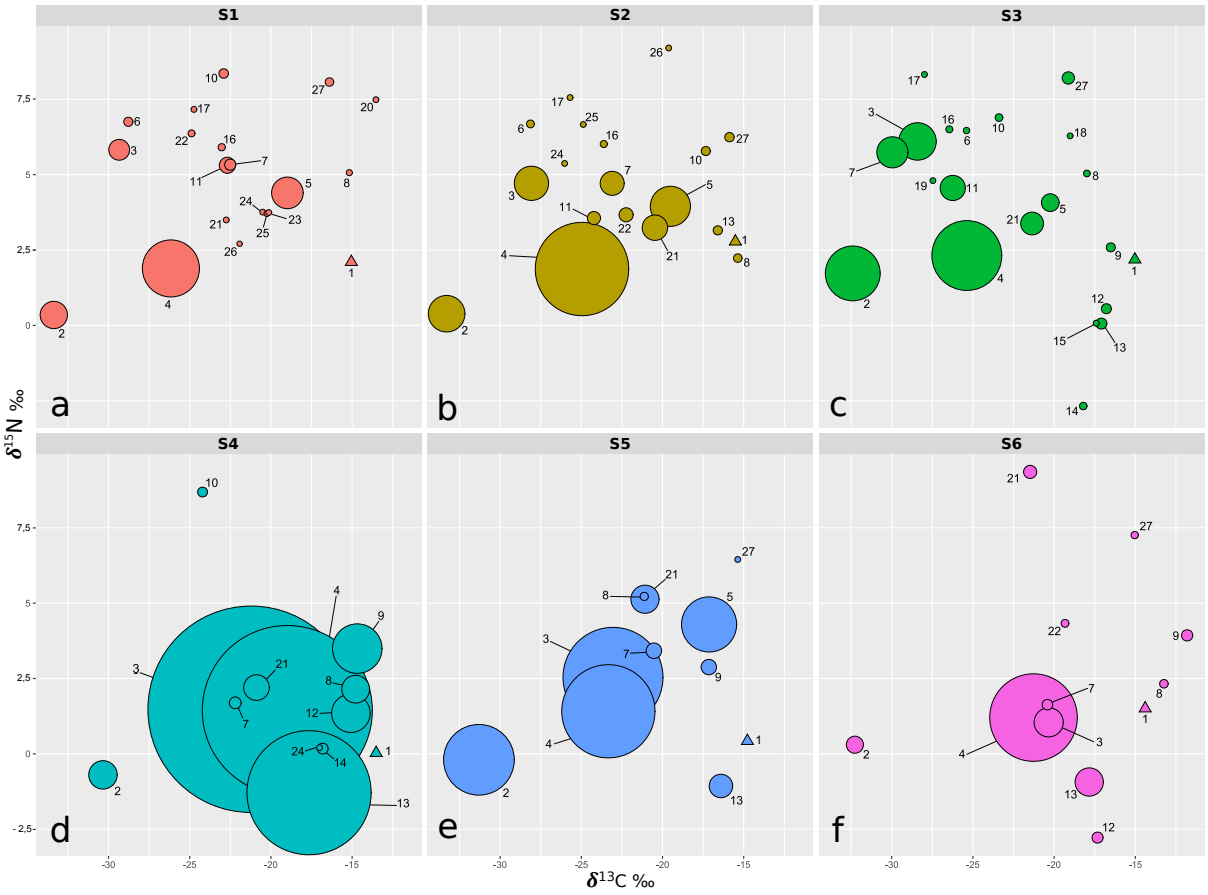

Figure 5. Stable isotope bi-plots showing vent consumers' isotope signatures weighted by biomass per cubic meter (filled circles) for the six vent assemblages (S1 to S6) sampled on the Grotto hydrothermal edifice. Considered as a habitat, the biomass of *Ridgeia piscesae* (denoted by a triangle symbol) is not shown. Each vent species is designated by a number: 1 = *Ridgeia piscesae*; 2 = *Provanna variabilis*; 3 = *Depressigyra globulus*; 4 = *Lepetodrilus fucensis*; 5 = *Buccinum thermophilum*; 6 = *Clypeosectus curvus*; 7 = *Amphisamytha carldarei*; 8 = *Branchinotogluma tunnicliffeae*; 9 = *Lepidonotopodium piscesae*; 10 = *Levensteiniella kincaidi*; 11 = *Nicomache venticola*; 12 = *Paralvinella sulfincola*; 13 = *Paralvinella palmiformis*; 14 = *Paralvinella pandorae*; 15 = *Paralvinella dela*; 16 = *Hesiospina sp. nov.*; 17 = *Sphaerosyllis ridgensis*; 18 = *Ophryotrocha globopalpata*; 19 = *Berkeleyia sp. nov.*; 20 = *Protomystides verenae*; 21 = *Sericosura* sp.; 22 = *Euphilomedes climax*; 23 = *Xylocythere sp. nov.*; 24 = Copepoda; 25 = *Copidognathus papillatus*; 26 = *Paralicella vaporalis*; 27 = *Helicoradomenia juani*. For legibility, the biomass of *P. pandorae* in collection S6 is not shown.

Table 1. Univariate measures of macrofaunal community structure associated with *Ridgeia piscesae* tubeworm bushes on the Grotto edifice: area, tube height, volume, species richness (S), exponential of Shannon entropy (D), Simpson's diversity index (1-λ') and Pielou's evenness (J').

Sample	Area (dm^2)	Tube height (dm)	Volume (dm^3)	S	D	1-λ'	J'
S1	12.36	1.724	21.313	28	5.377	0.728	0.505
S2	6.329	0.816	5.163	24	5.398	0.749	0.531
S3	11.921	1.789	21.328	31	6.053	0.778	0.524
S4	1.496	0.468	0.7	19	2.605	0.55	0.325
S5	1.558	0.553	0.862	19	4.348	0.697	0.499
S6	1.217	0.836	1.017	14	3.998	0.633	0.525

Table 2. Percentage abundance x 100 (% Ab.), volume (Vol. m^3) and relative biomass x 100 (% Biom.) of the different macrofaunal taxa (>250 µm) identified in the 6 sampling units (S1 to S6) on the Grotto edifice. The taxa were identified to the lowest possible taxonomical level.

Species	S1			S2			S3			S4			S5			S6		
	% Ab.	Vol. (m^3)	% Biom.	% Ab.	Vol. (m^3)	% Biom.	% Ab.	Vol. (m^3)	% Biom.	% Ab.	Vol. (m^3)	% Biom.	% Ab.	Vol. (m^3)	% Biom.	% Ab.	Vol. (m^3)	% Biom.
Annelida																		
Polychaeta																		
Sibogliinidae																		
Ridgeia piscesae	5.170	78789.301	80.021	16.272	845542.636	83.724	1.855	58274.730	72.575	7.532	1458571.429	58.582	7.496	559302.326	42.621	27.073	435294.118	78.038
Maldanidae																		
Nicomache venticola	0.105	1595.495	0.153	0.086	4457.364	0.080	0.225	7079.231	1.089	0	0	0	0	0	0	0	0	0
Dorvilleidae																		
Ophryotrocha globopalpata	0.055	844.674	< 0.001	0.060	3100.775	< 0.001	1.283	40318.800	< 0.001	0.007	1428.571	< 0.001	0.016	1162.791	< 0.001	0	0	0
Orbiniidae																		
Berkeleyia sp. nov.	0	0	0	0	0	0	0.040	1265.823	< 0.001	0	0	0	0	0	0	0	0	0
Hesionidae																		
Hesiospina sp. nov.	0.129	1970.906	0.016	0.063	3294.574	0.004	0.091	2859.822	0.007	0	0	0	0	0	0	0	0	0
Phyllodocidae																		
Protomystides verenae	0.006	93.853	< 0.001	0.004	193.798	< 0.001	0.001	46.882	< 0.001	0	0	0	0	0	0	0	0	0
Polynoidae																		
Branchinotogluma tunnicliffeae	0.009	140.779	0.002	0.056	2906.977	0.013	0.016	515.706	0.005	0.199	38571.429	0.241	0.031	2325.581	0.019	0.183	2941.176	0.027
Branchinotogluma sp.	0	0	0	0	0	0	0	0	0	0.007	1428.571	< 0.001	0	0	0	0	0	0
Lepidonotopodium piscesae	0	0	0	0.007	387.597	< 0.001	0.024	750.117	0.036	0.184	35714.286	0.936	0.078	5813.953	0.238	0.122	1960.784	0.092
Levensteinella kincaidi	0.108	1642.421	0.079	0.063	3294.574	0.017	0.025	797	0.015	0.015	2857.143	0.010	0.031	2325.581	< 0.001	0	0	0
Sigalionidae																		
Pholoe courtneyae	0.003	46.926	< 0.001	0	0	0	0	0	0	0	0	0	0	0	0	0	0	0
Syllidae																		
Sphaerosyllis ridgensis	3.387	51618.958	0.001	1.037	53875.969	< 0.001	1.668	52414.440	0.001	0	0	0	0.140	10465.116	< 0.001	0.061	980.392	< 0.001
Alvinellidae																		
Paralvinella dela	0	0	0	0	0	0	0.004	140.647	0.001	0	0	0	0	0	0	0	0	0
Paralvinella palmiformis	0	0	0	0.063	3294.574	0.019	0.066	2062.822	0.088	3.054	591428.571	6.775	0.171	12790.698	0.768	0.488	7843.137	1.413
Paralvinella pandorae	0.009	140.779	< 0.001	0.015	775.194	< 0.001	0.110	3469.292	0.013	0.074	14285.714	0.014	0.109	8139.535	< 0.001	3.963	63725.490	< 0.001
Paralvinella sulfincola	0	0	0	0	0	0	0.042	1312.705	0.059	0.516	100000	0.528	0.016	1162.791	< 0.001	0.122	1960.784	0.086
Ampharetidae																		
Amphisamytha carlottarei	25.404	387142.187	0.539	20.509	1065697.674	0.453	34.164	1073511.486	1.844	0.339	65714.286	0.020	4.675	348837.209	0.244	5.366	86274.510	0.069
Ctenodrilidae																		
Raricirrus sp.	0.003	46.926	< 0.001	0	0	0	0.012	375.059	< 0.001	0	0	0	0	0	0	0	0	0
Spionidae																		
Prionospio sp.	0.028	422.337	< 0.001	0	0	0	0.006	187.529	< 0.001	0	0	0	0	0	0	0	0	0
Mollusca																		
Aplacophora																		
Simrothiellidae																		
Helicoradomenia juani	3.467	52839.043	0.045	2.808	145930.233	0.020	5.474	172011.252	0.135	0.074	14285.714	< 0.001	1.231	91860.465	< 0.001	1.463	23529.412	0.010
Gastropoda																		
Buccinidae																		
Buccinum thermophilum	0.129	1970.906	3.220	0.112	5813.953	1.574	0.015	468.823	0.428	0	0	0	0.078	5813.953	5.809	0	0	0
Provannidae																		
Provanna variabilis	1.801	27451.901	2.249	1.367	71124.031	1.266	4.413	138677.918	6.780	0.258	50000	0.256	7.963	594186.047	10.003	1.280	20588.235	0.372
Peltospiridae																		
Depressigyra globulus	10.254	156264.664	1.117	12.095	628488.372	1.085	19.724	619784.341	2.861	47.488	9195714.286	13.016	40.736	3039534.884	20.979	16.951	272549.020	1.528
Clypeosectidae																		
Clypeosectus curvus	0.456	6945.096	0.066	0.123	6395.349	0.008	0.043	1359.587	0.003	0	0	0	0.078	5813.953	< 0.001	0	0	0
Lepetodrilidae																		
Lepetodrilus fucensis	40.539	617785.077	12.479	33.066	1718217.054	10.065	22.355	702437.881	11.528	39.764	7700000	19.425	27.863	2079069.767	18.100	40.122	645098.039	18.181
Arthropoda																		
Arachnida																		
Halacaridae																		
Copidognathus papillatus	4.597	70061.004	< 0.001	1.290	67054.264	< 0.001	4.794	150632.911	< 0.001	0.037	7142.857	< 0.001	0.001	6976.744	< 0.001	0	0	0
Amphipoda																		
Alicellidae																		
Paralicella cf. vaporalis	0.022	328.484	< 0.001	0.037	1937.984	< 0.001	0.019	609.470	< 0.001	0	0	0	0	0	0	0	0	0
Calliopiidae																		
Oradarea cf. walkeri	0.062	938.527	< 0.001	0	0	0	0	0	0	0	0	0	0	0	0	0	0	0
Letgamphopus sp.	0	0	0	0	0	0	0	0	0	0.015	2857.143	< 0.001	0	0	0	0	0	0
Crustacea																		
Philomedidae																		
Euphilomedes climax	0.684	10417.644	0.012	9.149	475387.597	0.100	0.148	4641.350	< 0.001	0.003	57142.857	< 0.001	0.094	624418.605	< 0.001	2.439	39215.686	0.016
Cytheruridae																		
Xylocythere sp. nov.	2.719	41435.946	< 0.001	1.145	59496.124	< 0.001	2.623	82419.128	< 0.001	0.030	5714.286	< 0.001	0.265	19767.442	< 0.001	0.061	980.392	< 0.001
Pycnogonida																		
Ammotheidae																		
Sericosura verenae	0.560	8540.591	< 0.001	0.515	2674.186	0.524	0.721	22644.163	0.844	935.873	20000	0.197	0.561	41860.465	1.221	0.305	4901.961	0.165
Sericosura venticola	0.200	3050.211	< 0.001	0.048	2519.380	0.524	0.012	375.059	0.844	66.848	1428.571	< 0.001	0	0	0	0	0	0
Sericosura cf. dissita	0.074	1126.232	< 0.001	0.007	387.697	0.524	0.004	140.647	0.844	0	0	0	0	0	0	0	0	0
Nemertea																		
Unidentified	0.015	234.632	< 0.001	0	0	0	0.018	562.588	< 0.001	0	0	0	0	0	0	0	0	0
Echinodermata																		
Ophiuroidae	0.003	46.926	< 0.001	0	0	0	0.003	93.765	< 0.001	0	0	0	0	0	0	0	0	0